

Identification, Localization, and Function in Steroidogenesis of PAP7: A Peripheral-Type Benzodiazepine Receptor- and PKA (R1 α)-Associated Protein

HUA LI, BABETT DEGENHARDT*, DEREK TOBIN, ZHI-XING YAO, KJETIL TASKEN, AND VASSILIOS PAPAPOPOULOS

Division of Hormone Research (H.L., B.D., Z.-X.Y., V.P.), Departments of Cell Biology, Pharmacology, and Neuroscience, Georgetown University School of Medicine, Washington, DC 20007; and Institute of Medical Biochemistry (D.T., K.T.), University of Oslo, N-0317 Oslo, Norway

Peptide hormones and cAMP acutely stimulate steroid biosynthesis by accelerating the transport of cholesterol into the mitochondria. The peripheral-type benzodiazepine receptor (PBR) has been shown to be an indispensable element of the cholesterol transport machinery. Using the yeast two-hybrid system and PBR as bait, we identified a protein that interacts with PBR, the PBR-associated protein PAP7. Using the regulatory subunit R1 α of PKA as bait, we also isolated PAP7. Glutathione-S-transferase -PAP7 interacted with both the mitochondrial PBR and cytosolic PKA-R1 α in MA-10 Leydig cells. PAP7 is a novel 52-kDa protein present in mouse, rat, and human tissues, and it has a major 3-kb mRNA transcript in all tissues examined. Immunohistochemical and *in situ* hybridization studies indicated that PAP7 is highly expressed in the gonads, adrenal, hippocampus,

and distinct brain neuronal and glial populations. Overexpression of the full length PAP7 increased the hCG-induced steroid production. However, overexpression of a partial PAP7, which includes the PBR- and PKA-R1 α -binding domains, inhibited the hormone-stimulated cholesterol transport and steroid synthesis. Treatment of MA-10 cells with oligonucleotides antisense to PAP7 also inhibited the hCG-stimulated steroid formation, suggesting that PAP7 is a functional element of the hormone-induced signal transduction cascade leading to steroidogenesis. PAP7 may function by targeting the PKA isoenzyme to organelles rich in PBR, *i.e.* mitochondria, where phosphorylation of specific protein substrates may induce the reorganization of PBR topography and function. (*Molecular Endocrinology* 15: 2211-2228, 2001)

PEPTIDE HORMONES SUCH as gonadotropins and ACTH act at their target tissues by binding to G protein-coupled cell surface receptors resulting in increased adenylate cyclase activity, increased cAMP levels, and activation of PKA. The resultant phosphorylation of specific protein substrates by PKA has been linked to increased steroid synthesis (1-4). Although PKA has broad substrate specificity, individual substrates may be specifically phosphorylated by particular pools of kinase compartmentalized at different subcellular loci through interaction with A kinase-anchoring proteins (AKAPs) (5, 6) that target PKA toward specific substrates. The PKA holoenzyme complex forms a tetramer consisting of two regulatory (R) and two catalytic (C) subunits. Four different regulatory subunits (R1 α , R1 β , R11 α , and R11 β) of PKA have

been identified and serve to regulate catalytic activity by binding and inactivating the C subunit. The C subunit is released and activated upon the binding of four molecules of cAMP to the R subunit dimer (7, 8).

The primary point of control in the acute stimulation of steroidogenesis by peptide hormones and cAMP involves the first step in this biosynthetic pathway where cholesterol is converted to pregnenolone by the C27 cholesterol side-chain cleavage cytochrome P-450 enzyme (P-450_{sc}) and auxiliary electron transferring proteins, localized on inner mitochondrial membranes (IMM) (2, 3). Detailed studies have shown that the rate-determining step in the hormone-stimulated steroid biosynthesis is the transport of the precursor, cholesterol, from intracellular sources to the IMM (2, 3). In our search for the structural elements participating in the mitochondrial uptake and transfer of cholesterol, we identified the peripheral-type benzodiazepine receptor (PBR) (9).

PBR is an 18-kDa protein, which was originally discovered because it binds the benzodiazepine diazepam with relatively high affinity (9). PBR, although present in all tissues examined, was found to be particularly high in steroid-producing tissues, where it

Abbreviations: AKAP, A kinase anchoring protein; AMG, aminoglutethimide; C subunit, catalytic subunit of PKA; DTT, dithiothreitol; GST, glutathione-S-transferase; HRP, horseradish peroxidase; IMM, inner mitochondrial membrane; OMM, outer mitochondrial membrane; PAP, PBR-associated protein; PBR, peripheral-type benzodiazepine receptor; RACE, rapid amplification of cDNA ends; R1 α , R1 β , R11 α , R11 β , regulatory subunits of PKA; SSC, sodium citrate/chloride buffer; StAR, steroidogenic acute regulatory protein.

was localized primarily in the outer mitochondrial membrane (OMM) (10). It was then demonstrated that PBR is a functional component of the steroidogenic machinery (11) mediating cholesterol delivery from the outer to the IMM (12). Further studies demonstrated that targeted disruption of the PBR gene in Leydig cells resulted in the arrest of cholesterol transport into mitochondria and steroid formation; transfection of the PBR-disrupted cells with a PBR cDNA rescued steroidogenesis (13). The role of PBR in cholesterol transport was further clarified by studies employing site-directed mutagenesis of PBR and *in vitro* expression (14). From these studies a region of the cytosolic carboxyl terminus of the receptor was identified as a cholesterol-binding site (14, 15). *In vivo* studies, in which adrenal and ovarian PBR levels were pharmacologically (16, 17) or developmentally (18) modulated, further demonstrated that the levels of PBR correlated with the ability of the steroidogenic tissues to form steroids.

The functional mitochondrial PBR is a multimeric receptor complex. It is composed of at least the 18-kDa isoquinoline binding protein, the 34-kDa voltage-dependent anion channel, and the adenine nucleotide carrier (19, 20). Further studies on the structure of the receptor indicated that the 18-kDa mitochondrial PBR protein is organized in clusters of four to six molecules. Addition of hCG to Leydig cells induces a rapid increase in PBR ligand binding (21) and morphological changes, namely, redistribution of PBR molecules in large clusters (22). These hCG-induced changes and steroid formation are inhibited by a PKA inhibitor (21, 22), suggesting the presence of a cAMP-inducible element regulating the PBR structure and function. In subsequent studies, using the R2C Leydig cell line, which produces high levels of steroids in a constitutive manner, we also observed that a cytosolic proteinaceous component regulated the ligand binding ability and function of the mitochondrial PBR (23).

Considering these observations, it seemed highly likely that other, probably cytoplasmic, proteins, may participate in or induce the formation of the active receptor complex. In this study, we applied the yeast two-hybrid technique and screened a mouse testis cDNA library using PBR as bait. We identified several proteins [PBR-associated proteins (PAPs)] that interacted with PBR. One such clone, named PAP7, showed high affinity for PBR, no sequence homology to any known entity, and a tissue distribution close to that of PBR. Interestingly, when screening a human lymphocyte library with the regulatory subunit RI α of PKA as bait, we also isolated PAP7 as a protein with *in vivo* selectivity for PKA-RI α . This finding suggests the presence of a signal transduction mechanism involving targeting of PKA by PAP7 to mitochondria rich in PBR. Furthermore, our results provide a good platform from which we can formulate a pathway by which PKA activity regulates steroidogenic proteins, such as the steroidogenic acute regulatory protein StAR (24), and reorganization of PBR topology and function, lead-

ing to cholesterol uptake and transport to the IMM. The cloning, characterization, tissue distribution, and function of PAP7 in the hormone-stimulated steroidogenesis are presented herein.

RESULTS

Isolation of PBR-Associated Proteins

We have used the MATCHMAKER Two-Hybrid System from CLONTECH Laboratories, Inc. (Palo Alto, CA) to clone genes whose products interact with the 18-kDa PBR protein. GAL4 (1–147)-PBR fusion (plasmid pGBT9 + PBR) was used as a bait to screen a mouse MATCHMAKER testis cDNA library constructed into the pGAD10 two-hybrid vector. About 3×10^6 transformants were tested, and five positive clones were obtained for their ability to interact with PBR. Library plasmids from these transformants were rescued in *Escherichia coli* strain DH5 α . Both the His⁺ phenotype and the expression of β -galactosidase were confirmed by a second-round transformation of strain HF7c carrying pGBT9-PBR (Table 1).

Plasmids from these positive clones were first analyzed by restriction enzyme digestion followed by nucleotide sequencing. Two clones were found to be coded by an unknown single gene, which because of its ability to interact with PBR was named PBR-associated protein 7 (PAP7). PAP7 was isolated in three independent screenings of the library (the nucleotide sequence for PAP7 has been deposited in the GenBank database under GenBank accession no. AF022770). The other two clones encoded different gene products, which we will address elsewhere. After performing 5'-rapid amplification of cDNA ends (RACE) and 3'-RACE, a full-length, composite PAP7 cDNA was assembled from sequencing both strands of the obtained clones and revealed an open reading frame encoding a 445-amino acid protein with a calculated molecular mass of about 52 kDa (Fig. 1). The amino acid sequence analysis showed that PAP7 has high percentages of glutamic acid (14%) and arginine residues (8.5%) and an acidic isoelectric point (pI) of 5.48. A Kyte-Doolittle hydrophathy plot analysis of the deduced amino acid sequence revealed that PAP7 is a hydrophilic protein with no typical transmembrane do-

Table 1. Identification of PAP7

	His3	β -Galactosidase Activity
PAP3	+	++
PAP7 (PAP17)	+	++
PAP20	+	++
Positive control	+	+++

Summary of the yeast two-hybrid screening of mouse testis library using the mouse PBR as bait. Details are presented in *Materials and Methods*. Results shown were reproduced in three independent experiments.

```

1  TCCATCCTAATACGACTCACTATAGGGCTCGAGCGGCCCGGGCAGGTCTCTGCTAACCCCTCTT
67  GGAGAGAGATGTGACTATAGAAAGGGTTGATTTGATGCGGAAGTTCGGGTGTCGGCGAGCGGAGGT
                                     M R K F R C R R A E V
133  GAGAGTAAAAGATGGCAAAGCCTTTCATCCAACCTTATGAAGAAAACTGAAGTTCGTGGCACTGCA
R V K D G K A F H P T Y E E K L K F V A L H
199  TAAGCAAGTTCTTTGGGCCCATATAACCCAGACACGTCCCCTGAGGTTGGATTCTTTGATGTGTT
K Q V L L G P Y N P D T S P E V G F F D V L
265  GGGGAATGATAGGAGGAGAGAATGGGCAGCTCTGGGAAACATGTCCAAGGAGGATGCCATGGTAGA
G N D R R R E W A A L G N M S K E D A M V E
331  GTTTGTGAAGCTTCTAAATAAGTGTGTCTCTCTCGGCATATGTTGCGTCCCACAGAATAGA
F V K L L N K C C P L L S A Y V A S H R I E
397  GAAGGAAGAAGAAGAGAAAAGAAAGCGGAGGAGGAGGCGAAGGCAGCGTGAAGAGGAAGAACG
K E E E E K R R K A E E E R R Q R E E E E R
463  AGAGCGGCTGCAAAAGGAAGAAGAGAAGCGGAAGCGAGAGGAGGAAGACCGGCTGAGACGGGAGGA
E R L Q K E E E K R K R E E E D R L R R E E
529  GGAAGAGAGGCGGCGGATAGAGGAAGAGAGGCTTCGGCTGGAACAGCAAAAGCAGCAGATAATGGC
E E R R R I E E E R L R L E Q Q K Q Q I M A
595  AGCTTFAAACTCGCAGACTGCCGTGCAATTCCAGCAGTATGCAGCCCAGCAGTATCCAGGGAACATA
A L N S Q T A V Q F Q Q Y A A Q Q Y P G N Y
661  CGAACACAGCAGATTCTCATCCGCCAGCTGCAGGAGCAGCACTATCAGCAGTATATGCAGCAGTT
E Q Q Q I L I R Q L Q E Q H Y Q Q Y M Q Q L
727  ATATCAAGTCCAGCTTGCACAACAACAGGCAGCATTACAGAAACAGCAAGAAGTAGTGTGGCTGG
Y Q V Q L A Q Q Q A A L Q K Q Q E V V M A G
793  GGCATCTGCCTGCATCATCAAAGGTGAACAGCTGGAGCAAGTGATACACTGTCAGTTAATGG
A S L P A S S K V N T A G A S D T L S V N G
859  ACAGGCCAAAACCCCACTGAAAATTCGAAAAAGTCCCTTGAGCCAGAAGCTGCAGAAGAAGCCTT
Q A K T H T E N S E K V L E P E A A E E A L
925  GGAATGGAACAAAGACTCTCTTCCAGTGATTGCAGCTCCATCCATGTGACAAGACCACAAAT
E N G P K D S L P V I A A P S M W T R P Q I
991  CAAAGACTTTAAAGAGAAGATTCGGCAGGATGCAGATTCTGTGATTACAGTACGTCGAGGGAAGT
K D F K E K I R Q D A D S V I T V R R G E V
1057  CGTCACCGTCCGAGTCCCAGTCAATGAGGAAGGATCATACTATTTTGGGAATTTGCCACAGACAG
V T V R V P T H E E G S Y L F W E F A T D S
1123  TTATGACATTGGGTTTGGGGTTTATTTTGAATGGACAGACTCTCCAAATGCTGCTGTGCTGTCAGTGTGCA
Y D I G F G V Y F E W T D S P N A A V S V H
1189  TGTCACTGAGTCCAGTGCAGGAGGAGGAGGAGGAAGAAAATGTCACCTGTGAAGAAAAAGCAAA
V S E S S D E E E E E E N V T C E E K A K
1255  AAAGAACGCCAACAAGCCTCTGCTGGATGAGATTGTACCTGTGTACCGGCGGGACTGTCACGAGGA
K N A N K P L L D E I V P V Y R R D C H E E
1321  AGTATATGCAGGCAGCCACCAGTATCCAGGGAGGGAGTCTATCTCCTCAAGTTTGATAATTCCTA
V Y A G S H Q Y P G R G V Y L L K F D N S Y
1387  CTCTCTGTGGAGTCCAAGTCCGTCTACTACAGAGTCTATTATACTAGATAGAGCTGCTGTTCAG
S L W R S K S V Y Y R V Y Y T R *
1453  GGTCCGGAGTCTAGGGTTGAGCACAACATGACGTTTAATTTCTTTGAAAAAAAAAAAAAAAAAAAA
1519  AAAAAAGCGCGCTGAATTCTAG

```

Fig. 1. Nucleotide and Predicted Amino Acid Sequence of the PAP7 cDNA

The complete nucleic acid sequence of the PAP7 cDNA (*top line*) and the deduced amino acid sequence of PAP7 protein (*bottom line*) are shown.

main. A homology search against the GenBank database using the BLAST program showed that this sequence has not been previously identified. A part of PAP7 shares quite high homology with a *Caenorhabditis elegans* gene that has an unknown function (25). PAP7 also shares limited homology with RALBP, a hydrophobic ligand-binding protein that functions in intracellular retinoid transport (26). By sequence motif analysis using Swiss-Prot Prosite profile scan, PAP7 was found to have fatty acylation (myristoylation) sites (G244, G253), acyl-coenzyme A (CoA)-binding protein signature (amino acid 8–90), bipartite nuclear targeting sequence (amino acid 132–149), and PKA (T326,

S436) and PKC (S95, S237, S262, T313, T321) phosphorylation sites.

Isolation of PAP7 as a PKA-Associated Protein

We used the two-hybrid assay to investigate protein interactions with the type I regulatory subunit of PKA. Full-length R1 α cDNA was used as bait to screen a normal human lymphocyte library (1×10^6 independent clones). Positive growth on histidine-deficient medium and β -galactosidase activity were used to identify positive protein-protein interactions, which resulted in the isolation of 13 positive clones. A clone

with strong growth and high β -galactosidase activity in the two-hybrid assay was shown to be a fragment of PAP7. Interestingly, the human sequence fragment was identical to the mouse sequence in nucleotides 736–1,207, which encodes amino acids 212–369 of the mouse PAP7.

We then cotransformed Y190 yeast cells with pGAD10-PAP7 together with the pAS2.1 vector fused with either RI α , RI β , RII α , or empty pAS2.1. Yeast transformed with both plasmids were selected by growth on Leu⁻/Trp⁻ plates. Double positive clones were then transferred by colony lift assay to selective medium (His⁻/Leu⁻/Trp⁻, with 20 mM 3-aminotriazole) to determine positive protein interaction. Further confirmation of protein interaction was provided by use of the β -galactosidase assay. As seen from Fig. 2, all plasmids were successfully introduced into Y190 yeast. Growth in His⁻ plates was seen only in yeast containing PAP7-RI α (not shown). Positive interaction was also assessed using the β -galactosidase assay from a colony lift directly from Leu⁻/Trp⁻ plates (Fig. 2). As seen, only yeast containing the PAP7-RI α showed positive interaction. Yeast containing RI β or RII α showed growth in Leu⁻/Trp⁻ but were not positive on His⁻ plates, or the β -galactosidase assay, indicating that, in yeast, the PAP7 does not bind to these subunits. Thus, in the two-hybrid assay PAP7 bound primarily to the RI α subunit of PKA and not to RI β or RII α .

PAP7 Protein Expression in MA-10 Leydig Tumor Cells

The presence of PAP7 in total MA-10 cell protein extracts was examined by immunoblotting using an anti-PAP7 antibody that we generated. This affinity-purified

antipeptide antibody specifically recognizes a 52-kDa protein band (Fig. 3A). No difference in the expression of the protein was seen between control and hCG-treated MA-10 cells. To demonstrate the specificity of the anti-PAP7 antibody developed, PC12 rat pheochromocytoma cells were transfected with the full-length PAP7 cDNA or empty vector. PC12 cells do not express immunoreactive PAP7 protein, whereas transfection with the PAP7 cDNA resulted in the expression of a 52-kDa immunoreactive protein (Fig. 3B). Preabsorbed antibody, with the peptide antigen used to generate and purify it, did not recognize the 52-kDa PAP7 protein (Fig. 3B). The PAP7 protein expression in MA-10 cells was also confirmed by immunocytochemistry in which the immunoreactivity was localized mainly in the cytoplasm (Fig. 3C, right). This signal could be neutralized by pretreating the antibody with the synthetic PAP7 peptide antigen (Fig. 3C, left).

In Vitro Binding of PAP7 to PBR and PKA

To verify the interaction between PAP7 and PBR or PKA-RI α , a fusion protein of glutathione-S-transferase (GST) with PAP7 (including amino acids 216–445) was bacterially produced and used in binding assays with MA-10 cytosolic and mitochondrial fractions. Because PBR is an integral OMM protein, we performed the GST-PAP7 (216–445) pull-down assay using solubilized mitochondria. Immunoblot analysis, using anti-PBR antibody, of the proteins obtained by incubation of MA-10 mitochondrial extracts with GST-PAP7 (216–445) followed by precipitation with glutathione-Sepharose 4B beads revealed that, indeed, PAP7 (216–445) interacts with PBR (Fig. 3, D and E). In control experiments, GST alone did not pull down the 18-kDa PBR protein (Fig. 3D). Immunoblot analysis,

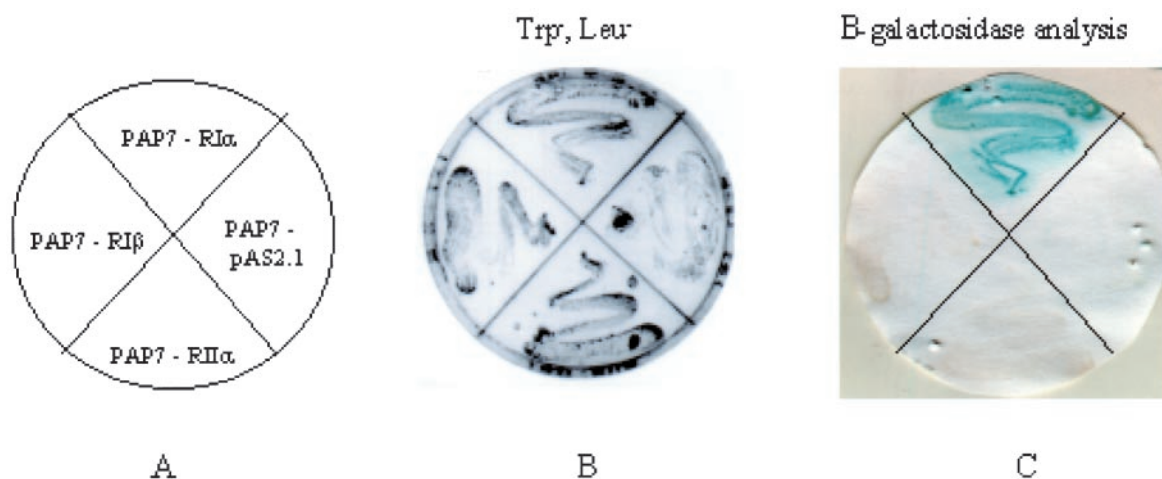


Fig. 2. Two-Hybrid Analysis of PAP7-R Subunit Interaction

Y190 yeast cells were cotransformed with either empty pAS2.1 or pAS2.1 fused either to RI α , RI β , or RII α and pGAD10-PAP7. A, Legend showing plating of yeast transformants. B, Yeast were plated onto Trp⁻, Leu⁻, to select for double positive transformants. C, Colony lift assay was performed from Trp⁻, Leu⁻, plate and β -galactosidase assay was performed. Blue indicates positive interaction between expressed proteins.

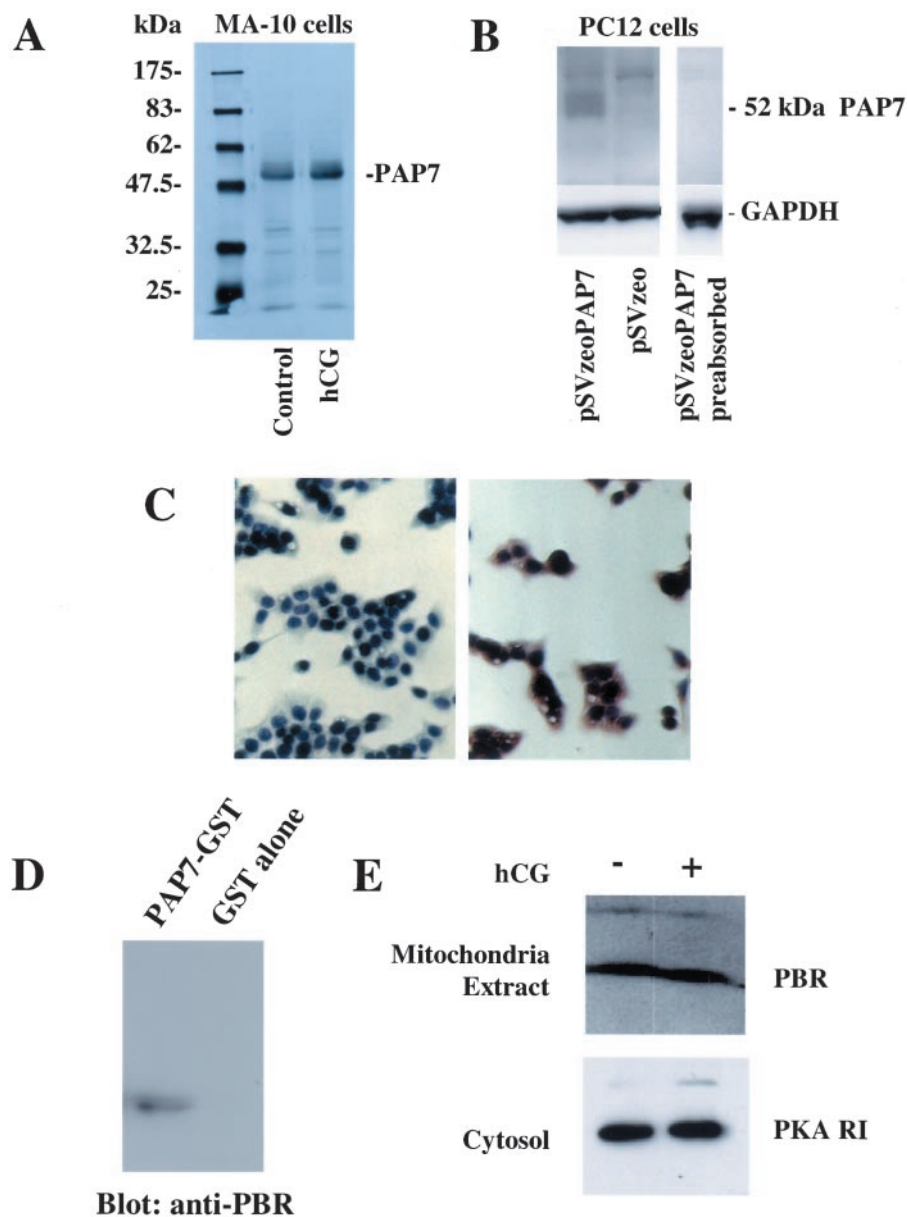


Fig. 3. Interaction of Recombinant PAP7 with PBR and PKARI in MA-10 Mouse Leydig Tumor Cells

A, Immunoblot analysis of MA-10 cell extracts from control cells and cells treated for 60 min with hCG (50 ng/ml) using affinity-purified anti-PAP7 peptide antiserum. B, Immunoblot analysis of PC12 cells transfected with either pSVzeoPAP7 full-length or pSVzeo vector. The membranes were incubated either with the anti-PAP7 antibody or with the antibody pretreated with the synthetic PAP7 peptide antigen used to generate and purify the antibody (preabsorbed). C, The plate on the *right* shows the PAP7 protein expressed in MA-10 mouse Leydig tumor cells identified by immunocytochemistry (positive reaction appears *brown*). The plate on the *left* shows the control where the antibody used was pretreated with the synthetic PAP7 peptide. Cells were counterstained with hematoxylin. D, MA-10 mitochondrial extracts were incubated with GST-PAP7 or GST alone. The protein complex formed was pulled down by incubating with glutathione-Sepharose beads and analyzed using 8–16% SDS-PAGE followed by immunoblot analysis using anti-PBR antisera. E, Mitochondrial and cytosolic extracts from control and hCG-treated MA-10 cells were incubated with GST-PAP7. The protein complexes formed were pulled down by incubating with glutathione-Sepharose beads and analyzed using 8–16% SDS-PAGE followed by immunoblot analysis using anti-PBR and anti-PKARI α or anti-PKARI β antisera. Similar results were obtained with both antisera. Results shown are with the anti-PKARI β antiserum, which detects both PKARI α and PKARI β .

using anti-PKA-RI antibody, of proteins obtained by incubation of MA-10 cytosolic fraction with GST-PAP7 (216–445), followed by precipitation with glutathione-

Sepharose 4B beads, demonstrated that PAP7 interacts with the RI subunit of PKA (Fig. 3E). No difference in the amount of immunoprecipitated PBR or RI could

be seen between control and hCG-treated MA-10 Leydig cells (Fig. 3E).

To determine the *in vitro* characteristics of PAP7 binding to the different regulatory subunits of PKA, we extended these initial GST-precipitation experiments. Recombinant PAP7-GST was purified from isopropyl- β -D-thiogalactopyranoside-stimulated *E. coli* and incubated with 50 nM of different recombinant R subunits. Equal loading of PAP7-GST and GST alone was determined from Coomassie blue-stained gels. As shown in Fig. 4, A and B, GST-PAP7, but not GST, precipitated RI α and RII α .

These *in vitro* results support those obtained in yeast showing that RI α binds directly to PAP7. The *in vitro* binding of RII α to PAP7 indicates interaction,

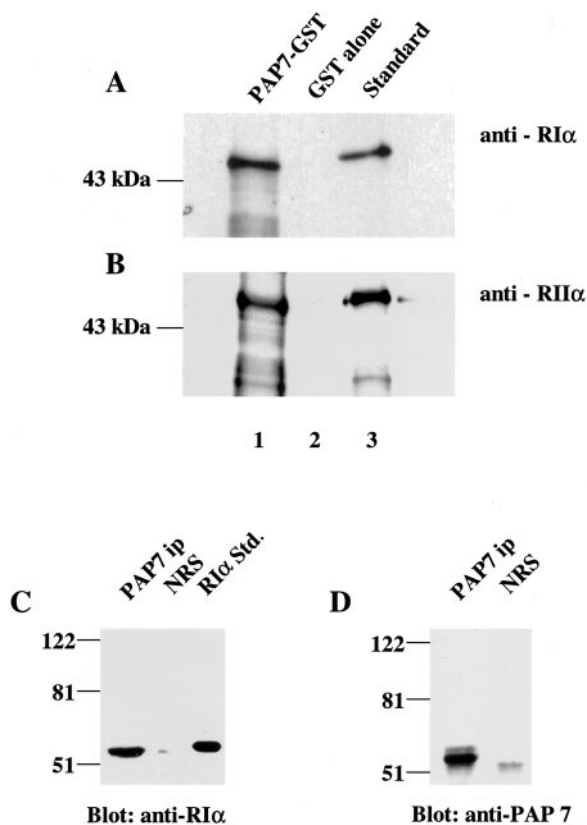


Fig. 4. PAP7 Binding to R Subunit by GST-Pull-Down and *In Vivo* Interaction of PAP7 with the RI α Subunit

Purified recombinant GST-PAP7 was incubated with recombinant R proteins. Complexes were precipitated by addition of glutathione beads, and Western blot analysis was performed using subunit-specific antibodies anti-PKARI α (panel A) and anti-PKARII α (panel B). Lane 1, PAP7-GST incubated with R subunit; lane 2, GST alone incubated with R subunit; lane 3, 20 ng of subunit-specific recombinant R subunit. Specific antibodies directed against the R subunit used in each experiment were employed. Immunoprecipitation of PAP7 from testis tissue and Western blotting for PKA R subunits. C, Western blot with RI α antibody. D, Membrane C was stripped and blotted for PAP7. PAP7 ip, PAP7 immunoprecipitation (ip); NRS, immunoprecipitation using normal rabbit serum; RI α std, 20 ng of recombinant RI α .

although this could not be shown in the yeast two-hybrid system. Furthermore, a somewhat weaker interaction was observed with RII β , but not with RI β (not shown). In addition, we performed further *in vitro* tests using a membrane overlay assay in which PAP7 was blotted to a membrane and incubated with a solution containing radiolabeled recombinant RI α or RII α . Using this method, both RI α and RII α again showed binding to PAP7 (results not shown) consistent with results from the GST-precipitation experiments.

Immunoprecipitation of PAP7 from Human Testis Tissue

To address the *in vivo* selectivity of R subunit interaction with PAP7, we performed immunoprecipitation of PAP7 from human testis tissue followed by immunoblot analysis for specific R subunits. As shown in Fig. 4, C and D, RI α is coimmunoprecipitated with PAP7 from human testis tissue. The reason for the different mobility of the recombinant RI α used as the standard and the immunoprecipitated RI α by the anti-PAP7 antibody is that the recombinant protein has a 17-amino acid extension, which changes the apparent SDS-PAGE mobility. In Fig. 4D the signal seen in the NRS lane is of lower size than PAP7 and probably corresponds to the light chain of the antibody used in the experiment. No coimmunoprecipitation of RII α was seen in agreement with the observations in the yeast-two hybrid system (not shown).

Tissue and Cell Expression of PAP7 Examined by RNA and Immunoblot Analyses

By dot blot analysis, PAP7 was present at high levels in brain, eye, submaxillary gland, testis, and ovary. Interestingly, PAP7 mRNA was present in embryos and decreased before birth (Fig. 5A). Consistent with these data, PAP7 mRNA was found by Northern blot analysis in adrenal, brain, heart, liver, testis, and ovarian tissues. PAP7 has a 3-kb major mRNA transcript in these tissues and an additional 1.7-kb transcript found only in testis (Fig. 5B). Preliminary data indicate that the 1.7-kb transcript is a spliced form present in the germ cells of the testis (data not shown). PAP7 mRNA was also abundant in three cell lines, C6 glioma, MA-10 Leydig, and Y1 adrenocortical (Fig. 5B), which have been widely used for studying the mechanisms regulating steroid biosynthesis. All three cell lines expressed the 3-kb PAP7 transcript. The PAP7 expression level in these cell lines was proportionally correlated with their steroidogenic ability. The PBR mRNA levels were also examined in these same tissues and cell lines. The levels of the 3-kb PAP7 message in the steroidogenic cell lines, MA-10, Y-1, and C6, parallel the PBR mRNA expression pattern (Fig. 5C). However, considering the cell-specific localization of PBR and PAP7 mRNAs, a correlation of their tissue expression levels cannot be determined by RNA (Northern) blot analysis.

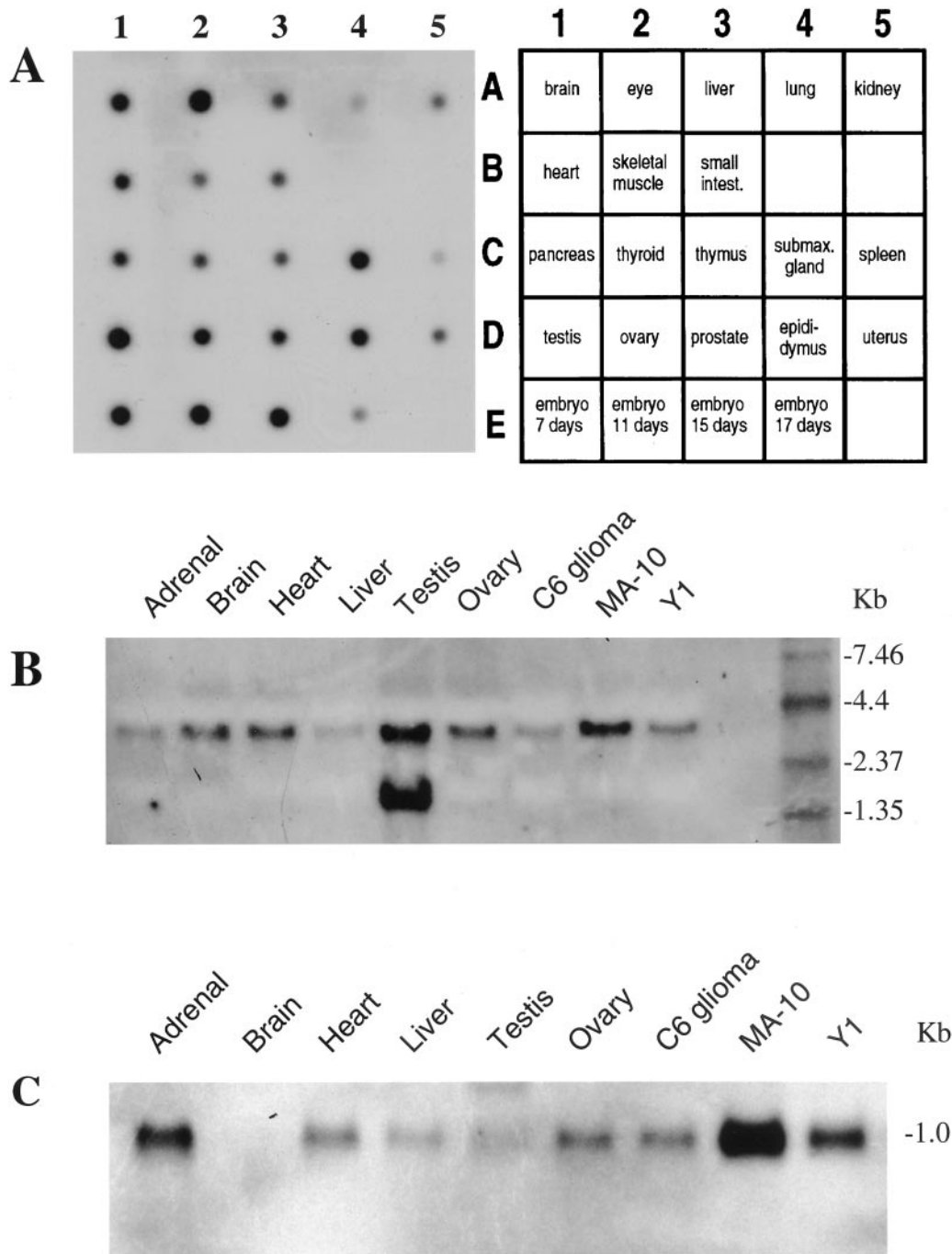


Fig. 5. PAP7 and PBR mRNA Tissue Distribution Analysis

A, Dot blot analysis of PAP7 mRNA expression. A Master blot containing 100–500 ng of poly(A)⁺ RNA from mouse tissues were hybridized at high stringency with a ³²P-labeled PAP7 probe as described in *Materials and Methods*. The autoradiogram was exposed overnight. RNA (Northern) blot analysis of PAP7 (panel B) and PBR (panel C) was performed using 20 μg of total RNA/lane from the indicated mouse tissues. The blot was hybridized at high stringency with a ³²P-labeled PAP7 probe as described in *Materials and Methods*. The autoradiogram was exposed overnight.

In addition, the PAP7 protein was identified in selected tissues (adrenal, testis, and ovary) by immunoblot analysis (data not shown). The molecular mass of the immunoreactive protein found in these tissues was 52 kDa, the same as seen for the MA-10 Leydig cells (Fig. 3A).

Tissue and Cell Distribution of PAP7 Examined by Immunohistochemistry and in Situ Hybridization

PAP7 protein expression in different tissues was investigated by immunohistochemistry (Fig. 6). PAP7

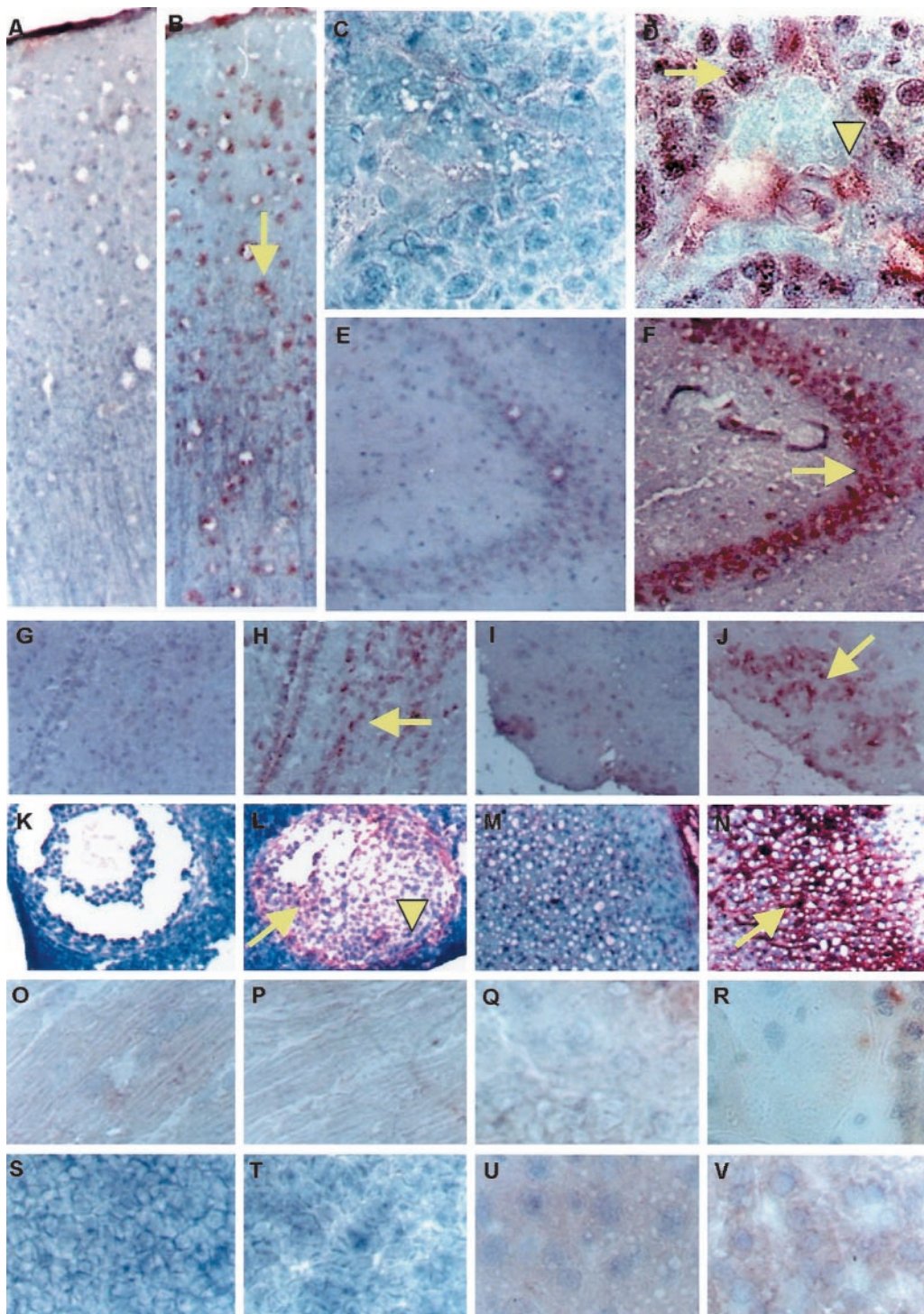


Fig. 6. PAP7 Expression in Mouse Tissues Examined by Immunohistochemistry

A, Brain negative control. B, Brain. C, Testis negative control. D, Testis. E, Brain hippocampus area negative control. F, Brain hippocampus area. G, Paraventricular nucleus negative control. H, Paraventricular nucleus. I, Superoptic nucleus negative control. J, Superoptic nucleus. K, Ovary negative control. L, Ovary. M, Adrenal negative control. N, Adrenal. O, Heart negative control. P, Heart. Q, Kidney negative control. R, Kidney. S, Spleen negative control. T, Spleen. U, Liver negative control. V, Liver. All negative controls shown were incubated with the anti-PAP7 antiserum preincubated with the peptide used to generate and purify the antibody. *Arrows* indicate cell-specific immunostaining in brain, germ cells of testis (D), granulosa cells of ovary (L), and adrenal fasciculata cells (N). *Arrowheads* indicate cell-specific immunostaining in Leydig cells of testis (D) and theca cells of ovary (L). Magnification, 100–400 \times .

was present in both Leydig and germ cells of the testis (Fig. 6D), in fasciculata reticularis and glomerulosa cells of the adrenal gland (Fig. 6N), and theca and granulosa cells of the ovary (Fig. 6L). In brain, PAP7 immunoreactivity was very strong in the hippocampus (Fig. 6F) and specific neuronal and glial cells of the cortex (Fig. 6B). Strong immunoreactivity was also found in the paraventricular (Fig. 6H) and superoptic nuclei (Fig. 6J) regions of the hypothalamus. Liver (Fig. 6V) and kidney (Fig. 6R) expressed low levels of PAP7 protein. Heart (Fig. 6P) and spleen (Fig. 6T) did not show any immunoreactivity for PAP7. Each specimen examined was also immunostained with the antibody preabsorbed with the peptide used to generate and isolate the antibody, as negative control (Fig. 6, A, C, E, G, I, K, M, O, Q, S, and U).

In situ hybridization studies indicated that PAP7 mRNA is also highly expressed in brain (Fig. 7, A and I) (hippocampus, olfactory bulb, neuronal and glial cells of the cortex), adrenal (Fig. 7C) (fasciculata and glomerulosa cells), ovary (Fig. 7E) (granulosa cells, theca cells at late stages, and primary follicles), and testis (Fig. 7G) (interstitial and tubular compartments) (Fig. 7). The PAP7 mRNA expression pattern seen in the tissues examined was closely related to that seen for the PAP7 protein (Fig. 6).

The Effect of PAP7 on Steroid Biosynthesis in MA-10 Cells

PAP7 full-length and partial sequence including the PBR and PKA-RI binding domains (contained in amino acids 228–445 and 212–369, respectively) were subcloned into pSVzeo mammalian expression vector. The pSVPAP7partial and pSVPAP7full-length vectors were transiently transfected into MA-10 cells. pSVzeo empty vector was also transfected into cells as control. The capability of steroid biosynthesis of the transfectants was examined by monitoring the progesterone production in response to hCG stimulation. PAP7 transfectants showed increased ability to form steroids in response to hCG (Fig. 8). This effect was statistically significant (unpaired t test; $P < 0.001$). In contrast, partial PAP7 (228–445) transfectants lost by 50–90% their ability to synthesize progesterone in response to saturating concentrations of hCG (Fig. 9A). This variability was probably due to the variability of the transfection efficiency (see Materials and Methods) suggesting that the dominant negative effect of the expressed PAP7 was present in all successfully transfected cells. However, the effect of the partial PAP7 (228–445) transfection on the hCG-stimulated steroid production was highly significant as shown by ANOVA ($P < 0.0001$). This effect was seen within 10 min upon addition of the hormone to the cells (Fig. 9B). However, under the same conditions the response in cAMP levels upon hCG treatment was similar in pSVzeo control transfectants and pSVPAP7partial transfectants (22 ± 2.3 vs. 24 ± 2.5 pmol/mg protein/2 h, $n = 6$).

To localize the site of action of the expressed full-length and partial PAP7, we then investigated their effect on the hCG-stimulated cholesterol transport. For that we used the aminoglutethimide-induced inhibition of P450_{scc} activity resulting in cholesterol accumulation within the mitochondria (12). Transfection of MA-10 cells with the full-length PAP7 followed by treatment with hCG resulted in a higher production of pregnenolone, reflecting increased accumulation of cholesterol at the IMM, compared with cells transfected with the empty vector (Fig. 10). However, transfection of MA-10 cells with the partial PAP7 inhibited pregnenolone formation by 70% (Fig. 10).

To further determine the role of PAP7 in the hormone-stimulated steroid synthesis, we treated MA-10 cells with oligonucleotides antisense to PAP7. To establish optimal conditions the fluorescein isothiocyanate-labeled antisense oligonucleotide was used, and preliminary dose-response and time course experiments were performed. At the end of the incubation, cells were washed and treated for 2 h with hCG (50 ng/ml). Results obtained using the optimal conditions of 72 h treatment with a concentration of 2 μ M oligonucleotides are shown. Treatment of the cells for 72 h reduced PAP7 protein levels by 75% and the ability of hCG to stimulate MA-10 progesterone synthesis (Fig. 11). Treatment with missense oligonucleotides inhibited PAP7 protein levels and steroid formation by 25% (Fig. 11). Treatment with antisense for 48 h inhibited PAP7 protein levels by 50% and the hCG-stimulated progesterone production. However, 48 h treatment with the missense had no effect on PAP7 levels and steroid production (not shown).

DISCUSSION

Despite the dramatic progress made in understanding the hormonal regulation of steroidogenesis (27), many questions remain unanswered. A number of these questions concern the identity of the signal transduction mechanism responsible for transducing the signal received from a small number of cAMP molecules to a maximally stimulated cholesterol transfer into mitochondria and steroid production by the cells within minutes. Although it has been clearly established that cAMP mediates the effect of hCG or LH on Leydig cell T synthesis, it is still puzzling that the concentrations of hCG needed to induce maximal cAMP synthesis are about 15 times larger than those needed to maximally stimulate T secretion (1). It is still unclear how these minimal cAMP levels could result in PKA-mediated activation of cholesterol transport and maximal steroid formation. In general, compartmentalization of cAMP and/or targeting of PKA via AKAPs could achieve such regulation. In our search of proteins involved in the transfer of cholesterol into mitochondria, we identified the 18-kDa PBR protein (9, 28). PBR is present in the central nervous system and various peripheral tissues,

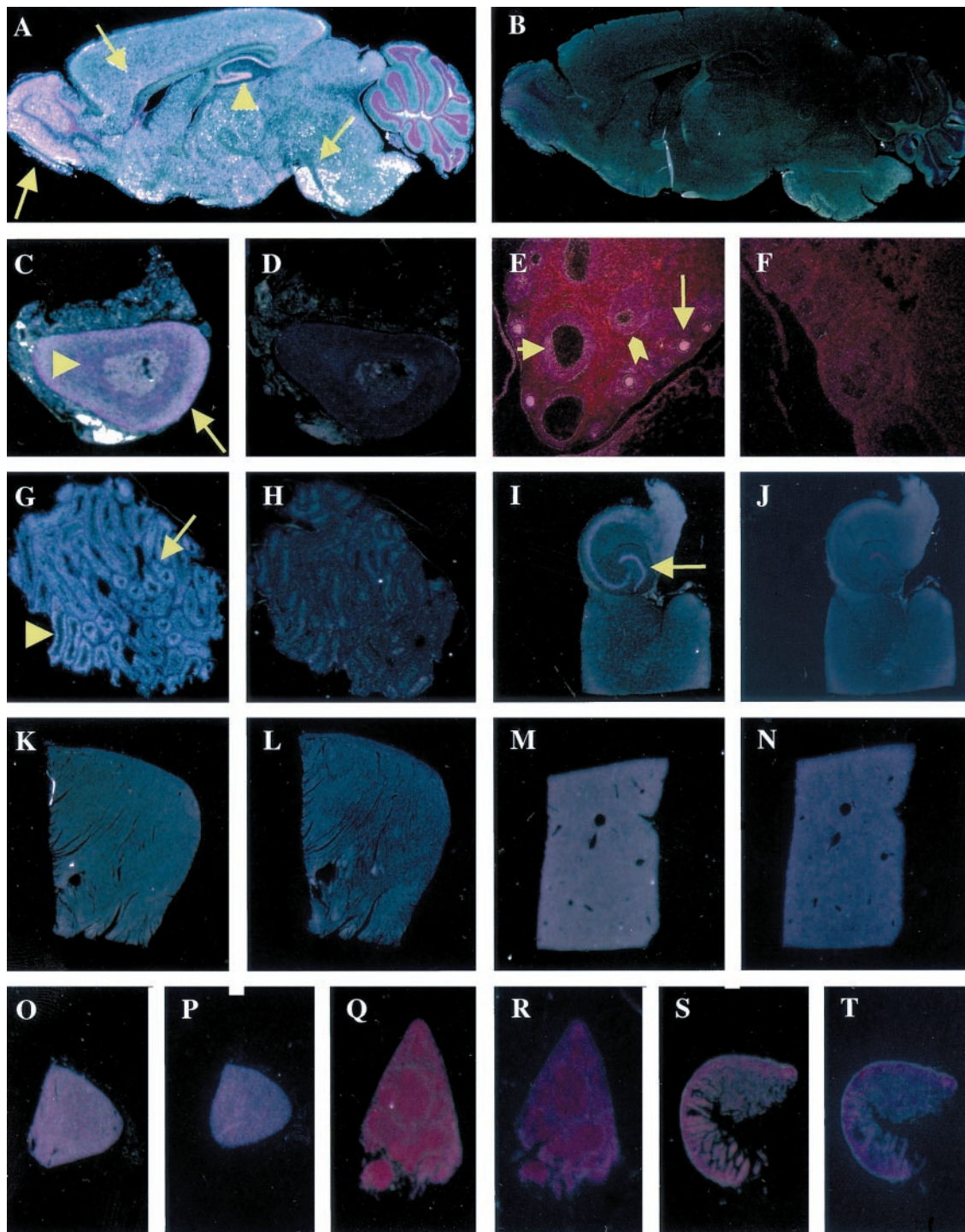


Fig. 7. mRNA Expression of PAP7 in Mouse Tissues Examined by *in Situ* Hybridization

Sections A, C, E, G, I, K, M, O, Q, and S were hybridized with an antisense ^{35}S -labeled cRNA probe to full-length PAP7. Sections B, D, F, H, J, L, N, P, R, and T were hybridized with sense probe. A and B, Brain sagittal section. C and D, Adrenal. E and F, Ovary. G and H, Testis. I and J, Brain coronal section. K and L, Heart. M and N, Liver. O and P, Kidney. Q and R, Spleen. S and T, Intestine. Slides were viewed under dark-field microscopy. Specific labeling, indicated by *arrows* and *arrowheads*, is seen as bright *white/pink* labeling. *Arrows* indicate cell-specific localization in brain (A and I), adrenal glomerulosa cells (C), granulosa cells and primary follicles in ovary (E), and Leydig cells of testis (G). *Arrowheads* indicate cell-specific localization in adrenal fasciculata-reticularis cells (C), theca cells in the ovary (E), and seminiferous epithelium of testis (G). Magnification, 40–100 \times .

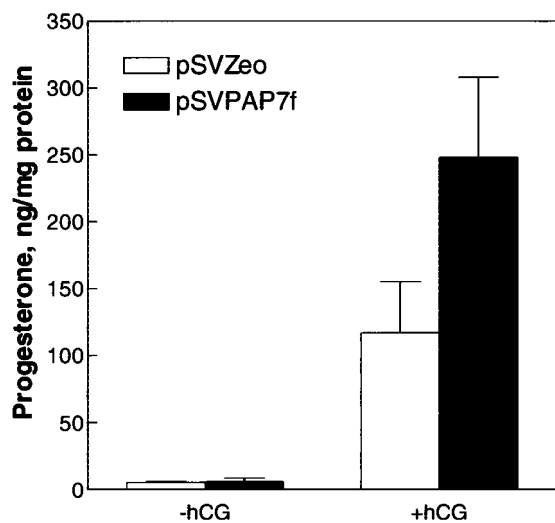


Fig. 8. Stimulatory Effect of the Full-Length PAP7 on Leydig Cell Steroidogenesis

MA-10 Leydig cells were transfected with either the pSVZeo vector alone or with the vector containing the full-length PAP7 insert (pSVPAP7f). Cells were then exposed to the saturating concentrations of hCG (50 ng/ml) for 2 h. At the end of the incubation media were collected and progesterone levels were determined by RIA. Results shown are means \pm SD from three independent experiments, each performed in triplicate.

including the testis, where it is expressed at high levels in Leydig cells (9, 28). Although the role of PBR in Leydig cell steroidogenesis has been well documented (9, 28), the mechanism by which hormones and cAMP may reach and regulate the mitochondrial PBR has not yet been identified. A series of studies has indicated that trophic hormones and cAMP, acting via PKA, regulate PBR ligand binding affinity and PBR distribution and function in cholesterol transfer into mitochondria and subsequent steroid formation (21–23). Furthermore, the presence of a proteinaceous cytosolic component, which could alter the PBR function, has been described in Leydig cells (23). The identity of this component is unknown. To better understand the mechanism underlying the hormonal regulation of PBR structure and function in cholesterol transport and steroidogenesis, we used the yeast two-hybrid assay to identify PBR-associated protein(s) in mouse testis Leydig cells. PAP7 was identified as a novel gene product present both in mouse and human, which demonstrated positive interaction with PBR. The PBR-PAP7 interaction was further verified using a GST pull-down assay using recombinant GST-PAP7 (216–445) fusion protein and solubilized MA-10 Leydig cell mitochondrial extracts, indicating that the PBR interaction domain resides in this region. Preliminary mutation deletion studies indicated that PAP7 interacts with the extramembrane hydrophilic domains of PBR (our unpublished results).

The distribution and expression of PAP7 were examined in several mouse tissues such as brain, testis,

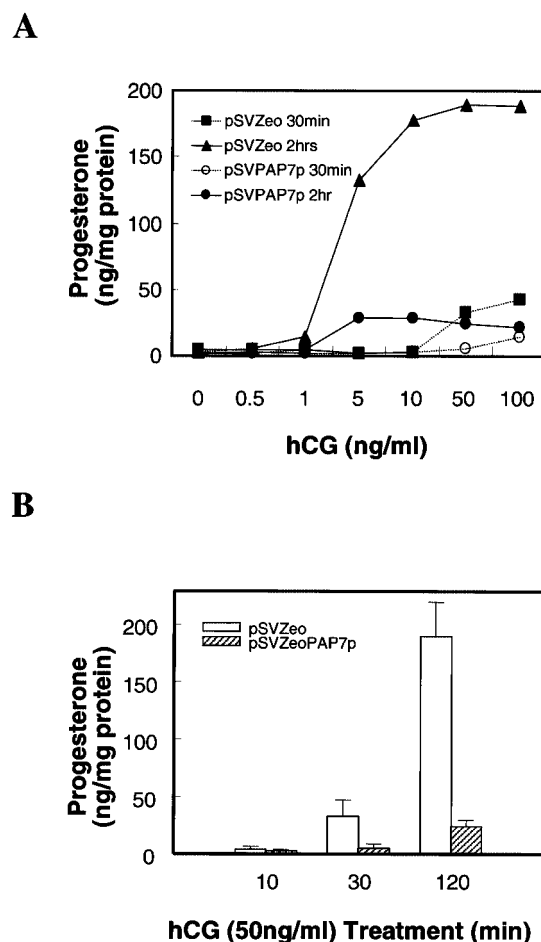


Fig. 9. Dominant-Negative Effect of the Partial PAP7 on Leydig Cell Steroidogenesis

MA-10 Leydig cells were transfected with either the pSVZeo vector alone or with the vector containing the partial PAP7 insert (pSVPAP7p). Cells were exposed to the indicated concentrations of hCG (A) for the indicated time periods (B). At the end of the incubation, media were collected and progesterone levels were determined by RIA. Results shown are means \pm SEM from three independent experiments, each performed in triplicate.

ovary, adrenal, and kidney, as well as steroidogenic cell lines. The PAP7 expression pattern is similar to the broader expression profile of PBR. In the testis, the Leydig cells are the sites of T biosynthesis. In the ovary, the theca and granulosa cells synthesize progestins and E. Glucocorticoids, androgen, and mineralocorticoids are produced by the zona fasciculata and glomerulosa cells of the adrenal. In the brain, glial cells (29, 30) and some neurons (31, 32) are able to synthesize neurosteroids. Interestingly, these are the sites at which PBR expression is very high in the body (9). In the brain, we found that PAP7 is abundant in the hippocampus and olfactory bulb. We have also found high levels of PBR in these areas (our unpublished data). The presence of steroidogenic enzymes in the olfactory bulb was recently shown (33), although its

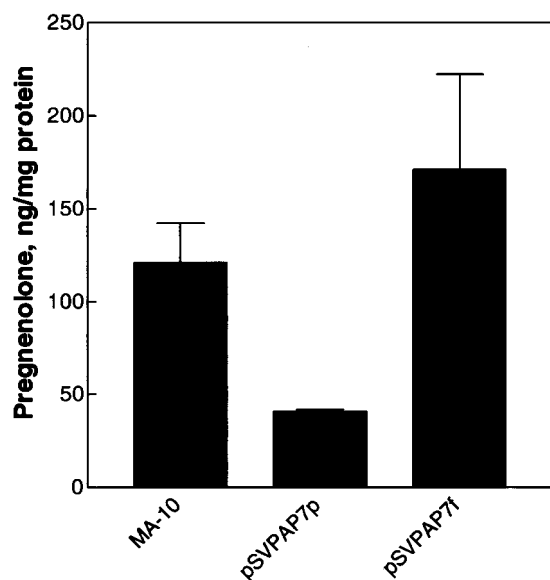


Fig. 10. The Effect of PAP7 Is Localized on Mitochondrial Cholesterol Transport

MA-10 Leydig cells were transfected with either the pSVzeo vector alone or with the vector containing the partial (pSVPAP7p) or full-length (pSVPAP7f) PAP7 insert. Cells were then exposed to the saturating concentrations of hCG (50 ng/ml) together with aminoglutethimide (0.5 mM) for 2 h. Mitochondria were prepared and the rate of pregnenolone formation in the absence of aminoglutethimide was measured as described in *Materials and Methods*. Results shown are means \pm SD from two independent experiments, each performed in triplicate.

ability to synthesize steroids is unknown. Moreover, it was recently shown that hippocampal neurons express steroidogenic enzymes and are able to synthesize specific neurosteroids (32). Our observations on the high level of PAP7 expression in these two brain areas complement these recent studies. In addition, high levels of PAP7 mRNA were found in rat C6 glioma cells, mouse MA-10 Leydig cells, and mouse Y1 adrenocortical cells, some of the most widely used cell models with which to study steroid biosynthesis. Because PAP7 is also highly expressed in these steroidogenic tissues, and considering its interaction with PBR, it is highly probable that PAP7 is involved in the regulation of steroid biosynthesis by changing the formation or the conformation of the mitochondrial PBR complex. In the testis, a second smaller PAP7 transcript, possibly due to alternative splicing or alternative use of polyadenylation site signals, was found. The presence of alternatively spliced genes is a common phenomenon in the testis (34, 35). Characterization of this transcript is under investigation in our laboratory.

It was recently reported that a protein named PRAX-1 specifically interacts with the carboxy terminus of PBR (36). PRAX-1 showed localization restricted to brain and thymus. Steroidogenic tissues, rich in PBR, were devoid of PRAX-1. The only similarity

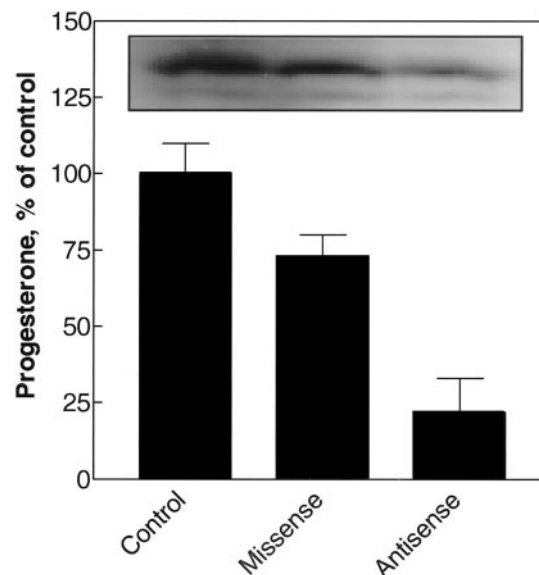


Fig. 11. Effect of Oligonucleotides Antisense to PAP7 on MA-10 Steroid Formation

MA-10 cells were treated with 2 μ M PAP7 antisense or missense oligonucleotides or vehicle for 72 h and then stimulated with hCG for 2 h. At the end of the incubation, media were collected and progesterone levels were determined by RIA. Results shown as percent of control are means \pm SD from three independent experiments, each performed in triplicate. In a representative experiment, cells were collected and PAP7 levels were determined by immunoblot analyses (*inset*).

between PAP7 and PRAX-1 is that both proteins contain glutamic acid stretches. Whether these stretches are critical for interacting with PBR remains to be determined. A part of PAP7 shares quite high homology with a *C. elegans* gene that has an unknown function (25). Interestingly, cholesterol is required for *C. elegans* cell culture (37). Considering that PBR is a cholesterol binding and channel-like protein (14, 15, 38, 39) and the PBR gene is highly conserved in all type of organisms, these data suggest that PAP7 expression may be needed to meet basic requirements for cell survival and growth. PAP7 also shares limited homology with RALBP, a hydrophobic ligand-binding protein that functions in intracellular retinoid transport (26).

PBR is a hydrophobic, integral protein of the OMM. Myristoylation and subsequent OMM translocation is one mechanism that, if present, could enable PAP7 to interact with PBR to transmit the signal generated by cAMP. Interestingly, the only known endogenous PBR ligand, the polypeptide diazepam binding inhibitor (9), is also an acyl-CoA-binding protein (40), suggesting that PAP7 may act as an endogenous PBR protein ligand. However, preliminary studies using MA-10 cells overexpressing PAP7 failed to show differences in PBR ligand binding (data not shown). The observation that PAP7 has potential protein kinase phosphorylation sites raises the possibility that PAP7 phosphorylation could facilitate its

interaction with PBR. Whether PAP7 phosphorylation is involved in its interaction with PBR is under investigation.

The finding that the regulatory subunit RI α of PKA also interacts with PAP7 in the yeast two-hybrid system indicated a link between cAMP, PKA, and PBR. The human PAP7 cDNA isolated in the yeast two-hybrid system screening using RI α was partial and encompassed amino acids 212–369, indicating that the binding domain for PKA resides in this area. Both RI α and RII α bind PAP7 in *in vitro* solution binding and filter overlay assays. However, results obtained from the GST-PAP7 (216–445) pull-down assays with MA-10 Leydig cell cytosolic fractions, immunoprecipitation of PAP7 from testis, as well as reconstitution in the two-hybrid system, showed interaction with RI α but not RII α or RII β . AKAP proteins normally interact with the RII subunit of PKA via an amphipathic helix region, and several such regions can be predicted in this area of PAP7. However, a further mutation/deletion analysis will be required for mapping of the interaction domain and understanding PKA isoenzyme selectivity, which may identify some determinants that favor interaction with RI α as recently described for other AKAP binding sites (41, 42).

Overexpression of the full-length PAP7 protein increased the hCG-stimulated steroid synthesis by MA-10 Leydig cells. However, overexpression of the PAP7 (228–445) fragment, which includes the PBR and PKA-RI α binding domains, inhibited hCG-stimulated progesterone formation in MA-10 Leydig cells. These data suggest that the overexpressed PAP7 (228–445) fragment acts as a competitor of endogenous PAP7 having a dominant-negative effect. Since this transfected PAP7 (228–445) fragment has a PBR and PKA-RI α binding domain, it may prevent PBR and/or PKA-RI from interacting with endogenous PAP7, thus inhibiting cholesterol accumulation into mitochondria and subsequent steroid formation. This also suggests that the transfected fragment of PAP7 (228–445) lacks, or has an ineffective, functional domain present in the wild-type protein. Detailed studies on the effect of PAP7 on the PBR ligand binding characteristics in response to hCG are in progress. In the same experiments, overexpression of the PAP7 (228–445) fragment did not alter the hCG-stimulated cAMP accumulation, indicating that the dominant negative effect seen is downstream of cAMP synthesis. This effect was subsequently localized at the level of cholesterol transport to P450 $_{scc}$. Overexpression of the full-length PAP7 increased and overexpression of the PAP7 (228–445) decreased the amount of cholesterol transported into the IMM, in response to hCG, available to P450 $_{scc}$ for pregnenolone synthesis. The role of PAP7 in the hormone-induced steroid formation was further demonstrated using oligonucleotides antisense to PAP7, which specifically inhibited the hCG-stimulated progesterone formation by MA-10 cells.

These studies demonstrate the presence of a cytosolic protein (PAP7) involved in the hormonal regulation of steroid formation, which interacts with both the cytosolic RI α subunit of PKA and the mitochondrial PBR. The association of PKA-RI with steroidogenic mitochondria has been reported (43). More specifically, it was shown in porcine ovaries that PKA activity is higher in mitochondria than cytosol. PKA-RI was then found to be predominant in the mitochondria whereas PKA-RII was predominant in the cytosol. Moreover, the mitochondrial PKA-RI to PKA-RII ratio was higher in corpora lutea, where there is maximal output of progesterone by the ovary (43). The importance of PKA-RI in Leydig cell steroidogenesis was also shown by Moger (44), who suggested that PKA type I is compartmentalized in Leydig cells so that it has preferential access to endogenously produced cAMP. The compartmentalization of PKA, mediated through the specific binding of R subunits to various organelles, has been recently proposed as a mechanism to target the response to cAMP (45). A dual RI/RII specificity PKA anchoring protein, which targets PKA to either mitochondria or endoplasmic reticulum, was recently described (45). In this article, we present evidence suggesting that PAP7 is a PKA-RI α anchoring protein targeting the kinase to mitochondria. Anchoring to the mitochondria could be accomplished via PAP7 myristoylation. There, PKA could phosphorylate specific protein substrates, such as StAR (24). StAR is a cytosolic hormone-induced protein implicated in the hormone-induced cholesterol transport into mitochondria (24). Phosphorylation of StAR has been shown to be responsible, in part, for the regulation of steroidogenesis by hormones (46). Although initial studies suggested that StAR needs to enter the mitochondria to exert its activity (47), subsequent studies demonstrated that its site of action resides outside the mitochondrion (48). The recent findings that the mitochondrial PBR is a high-affinity cholesterol-binding protein (49) and that StAR and PBR are closely associated in the OMM (50) suggest that a StAR-PBR interaction might be the key to the initiation of cholesterol transport into mitochondria. At the same time, PAP7 may serve as an anchoring protein to bring together many PBR molecules (22), thus allowing the creation of contact sites of the OMM and IMM and the translocation of cholesterol from the OMM, where cholesterol may be harbored in the PBR channel (14, 15, 38, 39), to the IMM where the cytochrome P450 $_{scc}$ is located. Thus, with the identification of PAP7, we may now have an explanation of how a small, transient increase in cAMP levels may trigger maximal activation of steroid formation: upon its targeting/anchoring via PAP7. The activated PKA, targeted by PAP7, would be able to act at critical subcellular locations, such as PBR-rich sites of the OMM. The phosphorylation of specific target proteins will initiate cholesterol transfer into mitochondria.

MATERIALS AND METHODS

Materials

[α -³²P]dCTP (specific activity, 3,000 Ci/mmol), [1,2,6,7-³H]progesterone (specific activity, 94.1 Ci/mmol), [*N*-methyl-³H]PK 11,195 (specific activity, 86.9 Ci/mmol), and [*N*-methyl-³H]Ro5–4864 (specific activity, 86.3 Ci/mmol), were obtained from NEN Life Science Products (Boston, MA). Purified hCG (batch CR-125 of biological potency 11,900 IU/mg) was a gift from the National Hormone and Pituitary Program, NIH (Rockville, MD). PK11195 and Ro5–4864 were obtained from Research Biochemicals International, Inc. (Natick, MA). Nitrocellulose (0.45 μ m) was from Hoefer Scientific (San Francisco, CA). Restriction enzymes were from Stratagene (La Jolla, CA) and New England Biolabs, Inc. (Beverly, MA). Cell culture supplies were purchased from Life Technologies, Inc. (Gaithersburg, MD). Tissue culture plasticware was from Corning, Inc. (Corning, NY). Electrophoresis reagents and materials were supplied from Bio-Rad Laboratories, Inc. (Hercules, CA). All other chemicals used were of analytical grade and were obtained from various commercial sources.

Strains and Media

The genotype of the *Saccharomyces cerevisiae* reporter strain HF7c is MATa, ura3–52, his3–200, lys2–801, ade2–101, trp1–901, leu2–3, 112, gal4–542, gal80–538, LYS2::GAL-HIS3, URA3::(GAL4 17-mers)₃-CYC1-lacZ (CLONTECH Laboratories, Inc.). Yeast strains were grown at 30 C in standard liquid YPD medium or minimal SD synthetic medium with appropriate supplement amino acids (CLONTECH Laboratories, Inc.).

Plasmids and Construction

The mouse PBR cDNA coding sequence was subcloned into pGBT9 (CLONTECH Laboratories, Inc.) at *Eco*RI and *Bam*HI sites (pGBT-PBR). The fusion site was verified by sequencing. Functional fusion PBR protein, expressed in yeast cells, was verified by PBR ligand binding assay. Mouse testis cDNA library was constructed in pGAD10 [LEU2, GAL4 (768–881)] (CLONTECH Laboratories, Inc.). Amplification of premade libraries was performed by growing the transformants on LB-agar-ampicillin and purifying the plasmid's DNA with the Plasmid Giga kit (QIAGEN, Valencia, CA). In the transfection experiments, PAP7 partial sequence (including 217-amino acid C-terminal sequence, from 228–445) and full-length PAP7 were inserted into pSVzeo vector (Invitrogen, Carlsbad, CA) at *Eco*RI and *Bam*HI sites and named as pSVPAP7p and pSVPAP7f accordingly.

Yeast Two-Hybrid Screening

The MATCHMAKER two-hybrid system (CLONTECH Laboratories, Inc.) was applied in this study (detailed in manufacturer's instruction book). Briefly, the yeast reporter host strain HF7c was simultaneously cotransformed with both pGBT-PBR and the mouse testis cDNA library in pGAD10 plasmid by using the lithium acetate high-efficiency method (51). Screening of a normal human lymphocyte library was also performed using the CLONTECH Laboratories, Inc. MATCHMAKER two-hybrid system. The full-length R1 α subunit of PKA was subcloned into pAS2.1 and cotransformed together with the cDNA library (CLONTECH Laboratories, Inc., catalog no. HL4014AB) into Y190 yeast cells. HIS positive clones were further selected by colony lift filter assay for β -galactosidase activity. Plasmid DNA was rescued in *E. coli* DH5 α from yeast cells. Plasmids were retransformed into yeast HF7c cells with plasmid pGBT-PBR to test for histidine pro-

totrophy and β -galactosidase activity (CLONTECH Laboratories, Inc. manual). The cDNA inserts from the positive clones were sequenced. The full-length PAP7 cDNA was obtained by using the 5'- and 3'-RACE kit from CLONTECH Laboratories, Inc.

Sequence Analysis

The ABI PRISM dyes terminator cycle sequencing ready reaction kit and sequencer (both from PE Applied Biosystems, Foster City, CA) were used for sequencing at the Lombardi Cancer Center Sequencing Core Facility (Georgetown University). DNA sequences were analyzed by using Entrez and BLAST program against GenBank Database (National Center for Biotechnology, National Library of Medicine, NIH, Bethesda, MD).

Cell Culture and Transient Transfection

Mouse MA-10 cells were grown in modified Waymouth's MB752/1 medium containing 15% horse serum, as described previously (11). Rat C6 glioma and mouse Y1 adrenal cortical cells were cultured in DMEM and DMEM F12, respectively, with 10% FBS (12, 29). MA-10 cells were transiently transfected by electroporation (52). Each Genepulser cuvette (0.4-cm gap, Bio-Rad Laboratories, Inc.) contained 8×10^6 cells in 350 μ l antibiotic-free complete Waymouth's growth medium (see above), plus 30 μ g plasmid DNA in 50 μ l of 0.1 \times Tris-EDTA. Cells in electroporation cuvettes were electroshocked at 330 V and at a capacitance of 950 μ Farads generated from Genepulser (Bio-Rad Laboratories, Inc.). The cells were placed immediately on ice for 10 min before plating into 96-well plates. Transfection efficiency was monitored by β -galactosidase staining and varied from 50 to 90% of the cells attached to the dishes.

PC12 rat pheochromocytoma cells were grown and maintained as we previously described (53). PC12 cells were transfected with either pSVzeoPAP7 full-length cDNA or empty vector using the lipofectAMINE 2000 reagent following the instructions suggested by the manufacturer (Life Technologies, Inc.).

Radioligand Binding Assays

³H-PK11195 and ³H-Ro5–4864 binding studies were performed as we described previously (11). The dissociation constant (K_d) and the number of binding sites (B_{max}) were determined by Scatchard plot analysis of the data using the LIGAND program (54).

RNA (Northern) Blot Analysis

Total tissue and cellular RNA was isolated by the acid guanidinium thiocyanate-phenol-chloroform extraction method using RNA STAT60 reagent (Tel-Test Inc., Friendswood, TX). RNA was separated by denaturing electrophoresis and transferred to a Nytran membrane (Schleicher & Schuell, Inc., Keene, NH). The RNA blots were hybridized with ³²P-labeled PAP7 cDNA probe generated from random priming (Roche Molecular Biochemicals, Indianapolis, IN) (16, 21). Autoradiography was performed by exposing Kodak X-Omat AR films (Eastman Kodak Co., Rochester, NY) to the blots at –80 C overnight.

Relative Expression Level Analysis

Mouse master blot from CLONTECH Laboratories, Inc. was used to analyze relative expression levels of PAP7 among 50 tissues and during development. Hybridization and probe

construction were performed as described above. The density of autoradiographs was analyzed and quantified using SigmaGel Software (SPSS, Inc., Chicago, IL).

Antibody Generation And Immuno (Western) Blot Analysis

Rabbit anti-PAP7 antibody was prepared by sequential immunization with a peptide (367–391) SSDEEEEEENVT-CEEKAKKNANKP of PAP7 protein, which was coupled to keyhole limpet hemocyanin. PAP7 antibodies were purified by an affinity resin containing the same peptide immobilized onto agarose (Bethyl Laboratories, Montgomery, TX). MA-10 cells were solubilized in sample buffer (25 mM Tris-HCl (pH 6.8), 1% SDS, 5% β -mercaptoethanol, 1 mM EDTA, 4% glycerol, and 0.01% bromophenol blue), boiled for 5 min, and loaded onto a 15% SDS-PAGE minigel (MiniProtein II System, Bio-Rad Laboratories, Inc.). Electrophoresis was performed at 25 mA/gel using a standard SDS-PAGE running buffer (25 mM Tris, 192 mM glycine, and 0.1% SDS). The proteins were electrophoretically transferred to a nitrocellulose membrane (Schleicher & Schuell, Inc.). The membrane was incubated in blocking TTBS (20 mM Tris/HCl, pH 7.5, 0.5 M NaCl, and 0.05% Tween-20) buffer containing 10% nonfat milk at room temperature for 1 h, followed by incubation with a primary antibody against PAP7 (1:2,000) for 2 h. The membrane was washed with TTBS three times for 10 min each time. After 1 h incubation with the secondary antibody, goat antirabbit IgG conjugated with horseradish peroxidase (HRP) (Transduction Laboratories, Inc., Lexington, KY), the membrane was washed with TTBS three times for 10 min each time. Specific protein bands were detected by chemiluminescence using the Renaissance Kit (DuPont-NEN Life Science Products, Wilmington, DE).

Immunocytochemistry

MA-10 cells were cultured on four-chambered SuperCell Culture Slides (Fisher Scientific, Pittsburgh, PA) and fixed with methanol at 4 C for 15 min. The fixed cells were incubated with PAP7 antibody (1:250 dilution) with or without PAP7 peptide for 1 h. After washing, the cells were incubated with HRP-conjugated goat antirabbit secondary antibody (Transduction Laboratories, Inc.) for 1 h. PAP7 staining was visualized with peroxidase using 3-amino-9-ethyl carbazole as a chromogen to yield a red reaction product. After counterstaining with hematoxylin, slides were dehydrated and permanently mounted.

Immunohistochemistry

Mouse tissues were freshly snap frozen in TISSUE TEK (Fisher Scientific, Wood Dale, IL) on dry ice. Specimens were fixed in cold methanol immediately after sectioning. The slides were then placed in a chamber containing acetone for 1 min at room temperature to remove the lipid droplets and then incubated in blocking solution (10% goat serum) (Zymed Laboratories, Inc., South San Francisco, CA) for 10 min. Subsequently, the slides were incubated with anti-PAP7 antibody (1:100) for 3 h at 37 C in a humid chamber, washed with PBS three times for 5 min each, incubated with HRP-conjugated goat antirabbit secondary antibody for 1 h at 37 C, and then washed with PBS as before. To amplify the signal the slides were treated with biotinyl-tyramide working solution (TSA-Indirect Tyramide Signal Amplification Kit) (NEN Life Science Products) for 10 min at room temperature, and then incubated with diluted streptavidin-HRP for 30 min at room temperature. After treatment with 3-amino-9-ethyl carbazole reagent for 1 h at 37 C for color staining, the sections were counterstained with hematoxylin, dehydrated, and permanently mounted. Slides were viewed and pictures taken

using an BX-40 microscope equipped with a PM20 camera system (Olympus Corp., Melville, NY).

GST Precipitation Assay

The PAP7 (216–445) partial cDNA encoding interaction domain was inserted into pGEX-6P-1 bacterial expression vector (Amersham Pharmacia Biotech, Arlington Heights, IL). The GST-fused PAP7 (216–445) proteins were expressed in *E. coli* induced by isopropyl- β -D-thiogalactopyranoside and purified with glutathione-Sepharose (Amersham Pharmacia Biotech). MA-10 mitochondria were prepared as previously described (12). The cytosol was collected and the mitochondria were further treated with HEPES/sucrose buffer (10 mM HEPES, pH 7.5, 320 mM sucrose) containing 0.5% digitonin to partially solubilize PBR.

Cytosol and mitochondria extracts were incubated with purified GST-PAP7 (216–445) in 1 ml of PBS (137 mM NaCl, 2.7 mM KCl, 4.3 mM $\text{Na}_2\text{HPO}_4 \cdot 7 \text{H}_2\text{O}$, 1.4 mM KH_2HPO_4) overnight at 4 C. Glutathione-Sepharose 4B was added and rotated for 30 min at 4 C. The beads were washed with cold PBS five times for 5 min each. The beads were then boiled in SDS-PAGE buffer (1% SDS, 1% mercaptoethanol, 10 mM Tris-HCl (pH 8.0), 20% glycerol, 0.05% bromophenol blue), and the proteins were separated on a 8–16% SDS-polyacrylamide gel and analyzed by Western blot using anti-PBR (see above) and anti-PKA-R1 antisera (Santa Cruz, CA). Purified PAP7 protein was also incubated with 2.5 μg of purified recombinant R subunits [RI α , RI β , RII α , RII β] prepared as previously described (55) in 100 μl of pull-down buffer (300 mM NaCl, 0.1% Triton X-100, 1 mM phenylmethylsulfonyl fluoride, 1 mM EDTA, 5 mM benzamidine, 5 mM dithiothreitol (DTT), 10 $\mu\text{g}/\text{ml}$ of antipain, chymostatin, leupeptin, and pepstatin A). Extracts were then incubated with 50 μl of glutathione beads (1:1 slush in pull-down buffer) for 30 min. Beads were subsequently washed, then boiled in SDS-PAGE buffer, and Western blot analysis was performed for the presence of R subunits. Monoclonal antibodies directed against human RI α and human RII α (catalog nos. P53620 and P55120, respectively; K. Tasken in collaboration with Transduction Laboratories, Inc., Lexington, KY) were used at a concentration of 1.0 $\mu\text{g}/\text{ml}$ for immunoblotting.

Immunoprecipitations

Human testis tissue was obtained from patients 65 to 75 yr of age in whom testes were removed as treatment for prostate cancer at the Department of Surgery, Ullevaal University Hospital, Oslo, Norway. Less than 5 min after removal, epididymis and rete testis were removed, testes were decapsulated, and pieces of testicular tissue were immediately frozen in liquid nitrogen. Testis tissue was crushed under liquid nitrogen using a pestle and mortar and suspended in sucrose buffer (250 mM sucrose, 10 mM KH_2PO_4 , 2 mM EDTA, 0.5% Triton X-100). Tissue was then homogenized three times for 20 sec and centrifuged in an Eppendorf centrifuge to remove the insoluble material. Immunoprecipitation was performed using 500 μg protein with anti-PAP7 antibody (1:100 dilution) overnight at 4 C. Twenty-five microliters of protein A/G plus agarose were then added for 1 h, after which the beads were washed, then boiled in SDS-loading buffer, and precipitates were submitted to Western blot analysis (as above).

In Situ Hybridization

In situ hybridization was performed according to Fox's protocol (56) by us and Molecular Histology Labs, Inc (Gaithersburg, MD). Briefly, slides were rehydrated in 10 mM DTT in PBS (30 min at 45 C), followed by 10 mM DTT-10 mM iodoacetamide-10 mM *N*-methyl maleimide in PBS (10 min at room temperature). Slides were rinsed in PBS (two times for 3 min),

acetylated (0.5% acetic anhydride in 0.1 M triethanolamine, pH 8.0, for 10 min), and rinsed in 2× sodium citrate/chloride buffer (SSC) for 10 min. Twenty-five microliters of prehybridization cocktail (2× SSC, 1× Denhardt's, 50 mM phosphate buffer, 50 mM DTT, 500 μg/μl of salmon sperm DNA, 250 μg/μl of tRNA, 5 μg/ml poly(dA), 100 μg/ml poly(A), 0.05 pmol/ml of randomer, 57% dextran/formamide) were applied to individual slides, which were coverslipped, incubated at room temperature for 1 h, heat denatured at 80 C for 2 min, and submersed in ice-cold 2× SSC. Slides were removed from the ice bath; ³⁵S-labeled cRNA probe was applied, covered, placed in a sealed humidified chamber, and incubated at 45 C overnight (hybridization cocktail contained 0.08 μl of probe per μl of prehybridization cocktail). Coverslips were removed, and slides were rinsed three times in 2× SSC (5 min each at room temperature). Slides were then incubated in 76% formamide-0.25× SSC-1.2 mM DTT-0.5 mM EDTA (two times for 30 min at 37 C), 0.25× SSC (10 min at 37 C), and ribonuclease (RNase) (RNase A, 25 μg/ml; RNase T1, 5 U/ml) in 0.5 M NaCl-1.2 mM DTT-0.01 M Tris-HCl (pH 7.4) for 40 min at 37 C. Slides were rinsed in 2× SSC (two times for 5 min), dehydrated through graded 0.3 M ammonium acetate-ethanol, and air dried. Slides were then dipped in Kodak NTB-3 photographic emulsion (Eastman Kodak Co., Rochester, NY) at 45 C, sealed in a light-tight box, and incubated at 4 C for 5 d. Slides were developed at 15 C in D-19 developer (Kodak) for 4 min, followed by fixation (Kodak) for 6 min. Slides were counterstained with hematoxylin and eosin, coverslipped with permount, and evaluated under bright- and dark-field microscopy.

Steroid Biosynthesis

Control or transfected MA-10 cells were plated into 96-well plates at the density of 2.5×10^4 cells per well for overnight. The cells were stimulated with 50 ng/ml hCG in 0.2 ml/well serum-free medium for 2 h. The culture medium was collected and tested for progesterone production by RIA using antiprogestosterone antisera (ICN Biochemicals, Inc., Costa Mesa, CA), following the conditions recommended by the manufacturer. Progesterone production was normalized by the amount of protein in each well. RIA data were analyzed using the MultiCalc software (EG&G Wallac, Inc., Gaithersburg, MD).

cAMP Assay

MA-10 cells, either empty, transfected with pSVzeo vector alone, or transfected with PAP7, were treated and incubated as described above. At the end of the incubation, ethanol (65% final concentration) was added to the samples. cAMP was measured using the cAMP [¹²⁵I] RIA system from Amersham Pharmacia Biotech.

Evaluation of Cholesterol Accumulation in Mitochondria Using R(+)-p-Aminoglutethimide (AMG)

Cells were incubated in culture medium containing 500 μM AMG and medium with and without hCG (50 ng/ml) for 2 h. Cells were harvested and mitochondria were purified in the presence of AMG as we previously described (12). Purified mitochondria were washed in an AMG-free buffer so that P450_{scc} could recover its function and metabolize the accumulated cholesterol. Mitochondria, at a concentration of 1 mg/ml, were then incubated in the presence of 15 mM isocitrate and 5 mM NADP for 15 min at 37 C. The reaction was stopped with ice-cold ethanol, and pregnenolone was extracted and measured by RIA (12).

Oligonucleotide Treatment

Antisense oligonucleotides and controls (missense and fluorescein isothiocyanate-labeled antisense) directed to PAP7 were designed and manufactured by Biognostik, Göttingen, Germany. The sequences were: antisense, TGGCCTGTC-CATTAAGT; randomized mismatch control with same AT/GC ratio (missense), GTCCCTATACGAAC. Cells were treated for various periods of time with increasing concentrations of oligonucleotides. At the end of the incubation cells were washed and treated for 2 h with hCG (50 ng/ml).

Protein Quantification and Statistical Analysis

Proteins were quantified by the dye-binding assay of Bradford (57) with BSA as the standard. Statistical analysis was performed by unpaired *t* test or ANOVA followed by the Student-Newman-Keuls test or the Dunnett multiple comparisons test using the InStat (v.3.0) package from GraphPad Software, Inc. (San Diego, CA).

Acknowledgments

We would like to thank the National Hormone and Pituitary Program (NICHD, NIH) for the hCG, Dr. B. Bregman for the analysis of the brain sections, and Drs. M. Culty and X. Yang for critically reviewing the manuscript.

Received July 6, 2000. Accepted August 14, 2001.

Address all correspondence and requests for reprints to: Dr. Vassilios Papadopoulos, Division of Hormone Research, Department of Cell Biology, Georgetown University School of Medicine, 3900 Reservoir Road, Washington, DC 20007. E-mail: papadopv@georgetown.edu.

This work was supported by NIH Grant HD-37032 from the National Institute of Child Health and Human Development (to V.P.) and by grants from the Norwegian Research Council, Norwegian Cancer Society, the European Union and Novo Nordic Research Foundation (to K.T.).

* On leave from the Institute of Pharmaceutical Biology, Martin-Luther-University Halle-Wittenberg, Halle/Saale, Germany.

REFERENCES

1. Catt KJ, Harwood JP, Clayton RN, Davies TF, Chan V, Katikineni M, Nozu K, Dufau ML 1980 Regulation of peptide hormone receptors and gonadal steroidogenesis. *Recent Prog Horm Res* 36:557–662
2. Simpson ER, Waterman MR 1983 Regulation by ACTH of steroid hormone biosynthesis in the adrenal cortex. *Can J Biochem Cell Biol* 61:692–707
3. Jefcoate CR, McNamara BC, Artemenko I, Yamazaki T 1992 Regulation of cholesterol movement to mitochondrial cytochrome P450_{scc} in steroid hormone synthesis. *J Steroid Biochem Mol Biol* 43:751–767
4. Hansson V, Skälhegg BS, Tasken K 1999 Cyclic-AMP-dependent protein kinase (PKA) in testicular cells. Cell specific expression, differential regulation and targeting of subunits of PKA. *J Steroid Biochem Mol Biol* 69: 367–378
5. Colledge M, Scott JD 1999 AKAPs: from structure to function. *Trends Cell Biol.* 9:216–221
6. Rubin CS 1994 A kinase anchor proteins and the intracellular targeting of signals carried by cyclic AMP. *Biochim Biophys Acta* 1224:467–479
7. Taylor SS, Knighton DR, Zheng J, Ten EL, Sowadski JM 1992 Structural framework for the protein kinase family. *Annu Rev Cell Biol* 8:429–462

8. Francis SH, Corbin JD 1994 Structure and function of cyclic nucleotide-dependent protein kinases. *Annu Rev Physiol* 56:237–272
9. Papadopoulos V 1993 Peripheral-type benzodiazepine/diazepam binding inhibitor receptor: biological role in steroidogenic cell function. *Endocr Rev* 14:222–240
10. Anholt RR, Pedersen PL, De SE, Snyder SH 1986 The peripheral-type benzodiazepine receptor. Localization to the mitochondrial outer membrane. *J Biol Chem* 261:576–583
11. Papadopoulos V, Mukhin AG, Costa E, Krueger KE 1990 The peripheral-type benzodiazepine receptor is functionally linked to Leydig cell steroidogenesis. *J Biol Chem* 265:3772–3779
12. Krueger KE, Papadopoulos V 1990 Peripheral-type benzodiazepine receptors mediate translocation of cholesterol from outer to inner mitochondrial membranes in adrenocortical cells. *J Biol Chem* 265:15015–15022
13. Papadopoulos V, Amri H, Li H, Boujrad N, Vidic B, Garnier M 1997 Targeted disruption of the peripheral-type benzodiazepine receptor gene inhibits steroidogenesis in the R2C Leydig tumor cell line. *J Biol Chem* 272:32129–32135
14. Li H, Papadopoulos V 1998 Peripheral-type benzodiazepine receptor function in cholesterol transport. Identification of a putative cholesterol recognition/interaction amino acid sequence and consensus pattern. *Endocrinology* 139:4991–4997
15. Li H, Yao Z, Degenhardt B, Teper G, Papadopoulos V 2001 Cholesterol binding at the cholesterol recognition/interaction amino acid consensus (CRAC) of the peripheral-type benzodiazepine receptor and inhibition of steroidogenesis by an HIV TAT-CRAC peptide. *Proc Natl Acad Sci USA* 98:1267–1272
16. Amri H, Ogwuegbu SO, Boujrad N, Drieu K, Papadopoulos V 1996 *In vivo* regulation of peripheral-type benzodiazepine receptor and glucocorticoid synthesis by Ginkgo biloba extract EGB 761 and isolated ginkgolides. *Endocrinology* 137:5707–5718
17. Sridaran R, Philip GH, Li H, Culty M, Liu Z, Stocco DM, Papadopoulos V 1999 GnRH agonist treatment decreases progesterone synthesis, luteal peripheral benzodiazepine receptor mRNA, ligand binding and steroidogenic acute regulatory protein expression during pregnancy. *J Mol Endocrinol* 22:45–54
18. Zilz A, Li H, Castello R, Papadopoulos V, Widmaier EP 1999 Developmental expression of the peripheral-type benzodiazepine receptor and the advent of steroidogenesis in rat adrenal glands. *Endocrinology* 140:859–864
19. McEnery MW, Snowman AM, Trifiletti RR, Snyder SH 1992 Isolation of the mitochondrial benzodiazepine receptor: association with the voltage-dependent anion channel and the adenine nucleotide carrier. *Proc Natl Acad Sci USA* 89:3170–3174
20. Garnier M, Dimchev AB, Boujrad N, Price JM, Musto NA, Papadopoulos V 1994 *In vitro* reconstitution of a functional peripheral-type benzodiazepine receptor from mouse Leydig tumor cells. *Mol Pharmacol* 45:201–211
21. Boujrad N, Gaillard JL, Garnier M, Papadopoulos V 1994 Acute action of choriogonadotropin on Leydig tumor cells: induction of a higher affinity benzodiazepine-binding site related to steroid biosynthesis. *Endocrinology* 135:1576–1583
22. Boujrad N, Vidic B, Papadopoulos V 1996 Acute action of choriogonadotropin on Leydig tumor cells: changes in the topography of the mitochondrial peripheral-type benzodiazepine receptor. *Endocrinology* 137:5727–5730
23. Garnier M, Boujrad N, Ogwuegbu SO, Hudson Jr JR, Papadopoulos V 1994 The polypeptide diazepam-binding inhibitor and a higher affinity mitochondrial peripheral-type benzodiazepine receptor sustain constitutive steroidogenesis in the R2C Leydig tumor cell line. *J Biol Chem* 269:22105–22112
24. Stocco DM 1999 Steroidogenic acute regulatory (StAR) protein: what's new? *Bioessays* 21:768–775
25. Wilson R, Ainscough R, Anderson K, Baynes C, Berks M, Bonfield J, Burton J, Connell M, Copsey T, Cooper J 1994 2.2 Mb of contiguous nucleotide sequence from chromosome III of *C. elegans*. *Nature* 368:32–38
26. Ozaki K, Terakita A, Ozaki M, Hara R, Hara T, Hara-Nishimura I, Mori H, Nishimura M 1994 Molecular characterization and functional expression of squid retinal-binding protein. A novel species of hydrophobic ligand-binding protein. *J Biol Chem* 269:3838–3845
27. Huhtaniemi I, Toppari J 1995 Endocrine, paracrine and autocrine regulation of testicular steroidogenesis. *Adv Exp Med Biol* 377:33–54
28. Papadopoulos V 1998 Structure and function of the peripheral-type benzodiazepine receptor in steroidogenic cells. *Proc Soc Exp Biol Med* 217:130–142
29. Papadopoulos V, Guarneri P, Krueger KE, Guidotti A, Costa E 1992 Pregnenolone biosynthesis in C6-2B glioma cell mitochondria: regulation by a mitochondrial diazepam binding inhibitor receptor. *Proc Natl Acad Sci USA* 89:5113–5117
30. Jung-Testas I, Hu ZY, Baulieu EE, Robel P 1989 Neurosteroids: biosynthesis of pregnenolone and progesterone in primary cultures of rat glial cells. *Endocrinology* 125:2083–2091
31. Ukena K, Usui M, Kohchi C, Tsutsui K 1998 Cytochrome P450 side-chain cleavage enzyme in the cerebellar Purkinje neuron and its neonatal change in rats. *Endocrinology* 139:137–147
32. Kawato S, Kimoto T, Takahashi T, Ohta Y, Tsurugizawa T, Makino J, Hojo Y, Takahashi T 2000 Localization and activities of neurosteroidogenic systems in the hippocampal neurons. In: Okamoto M, Ishimura YS, Nawata H, eds. *Molecular steroidogenesis*. Tokyo: Universal Academy Press Inc.; 385–392
33. Ohnishi T, Furukawa A, Tomita S, Miyatake A, Ichikawa, Y 2000 Co-localization of steroidogenic enzymes in the brain. In: Okamoto M, Ishimura YS, Nawata H, eds. *Molecular steroidogenesis*. Tokyo: Universal Academy Press, Inc.; 393–396
34. Zhang FP, Rannikko AS, Manna PR, Fraser HM, Huhtaniemi IT 1997 Cloning and functional expression of the luteinizing hormone receptor complementary deoxyribonucleic acid from the marmoset monkey testis: absence of sequences encoding exon 10 in other species. *Endocrinology* 138:2481–2490
35. Mauduit C, Chatelain G, Magre S, Brun G, Benahmed M, Michel D 1999 Regulation by pH of the alternative splicing of the stem cell factor pre-mRNA in the testis. *J Biol Chem* 274:770–775
36. Galiegue S, Jbilo O, Combes T, Bribes E, Carayon P, Le Fur G, Casellas P 1999 Cloning and characterization of PRAX-1. A new protein that specifically interacts with the peripheral benzodiazepine receptor. *J Biol Chem* 274:2938–2952
37. Brenner S 1974 The genetics of *Caenorhabditis elegans*. *Genetics* 77:71–94
38. Bernassau JM, Reversat JL, Ferrara P, Caput D, Lefur G 1993 A 3D model of the peripheral benzodiazepine receptor and its implication in intra mitochondrial cholesterol transport. *J Mol Graph* 11:236–44, 235
39. Culty M, Li H, Boujrad N, Amri H, Vidic B, Bernassau JM, Reversat JL, Papadopoulos V 1999 *In vitro* studies on the role of the peripheral-type benzodiazepine receptor in steroidogenesis. *J Steroid Biochem Mol Biol* 69:123–130
40. Knudsen J, Mandrup S, Rasmussen JT, Andreassen PH, Poulsen F, Kristiansen K 1993 The function of acyl-CoA-binding protein (ACBP)/diazepam binding inhibitor (DBI). *Mol Cell Biochem* 123:129–138
41. Angelo RG, Rubin CS 2000 Characterization of structural features that mediate the tethering of *Caenorhabditis elegans* protein kinase A to a novel A kinase anchor

- protein. Insights into the anchoring of PKAI isoforms. *J Biol Chem* 275:4351–4362
42. Miki K, Eddy EM 1999 Single amino acids determine specificity of binding of protein kinase A regulatory subunits by protein kinase A anchoring proteins. *J Biol Chem* 274:29057–29062
 43. Dimino MJ, Bieszczyk RR, Rowe MJ 1981 Cyclic AMP-dependent protein kinase in mitochondria and cytosol from different-sized follicles and corpora lutea of porcine ovaries. *J Biol Chem* 256:10876–10882
 44. Moger WH 1991 Evidence for compartmentalization of adenosine 3',5'-monophosphate (cAMP)-dependent protein kinases in rat Leydig cells using site-selective cAMP analogs. *Endocrinology* 128:1414–1418
 45. Huang LJ, Durick K, Weiner JA, Chun J, Taylor SS 1997 Identification of a novel protein kinase A anchoring protein that binds both type I and type II regulatory subunits. *J Biol Chem* 272:8057–8064
 46. Arakane F, King SR, Du Y, Kallen CB, Walsh LP, Watari H, Stocco DM, Strauss JF 1997 Phosphorylation of steroidogenic acute regulatory protein (StAR) modulates its steroidogenic activity. *J Biol Chem* 272:32656–32662
 47. Stocco DM, Clark BJ 1996 Regulation of the acute production of steroids in steroidogenic cells. *Endocr Rev* 17:221–244
 48. Arakane F, Sugawara T, Nishino H, Liu Z, Holt JA, Pain D, Stocco DM, Miller WL, Strauss III JF 1996 Steroidogenic acute regulatory protein (StAR) retains activity in the absence of its mitochondrial import sequence: implications for the mechanism of StAR action. *Proc Natl Acad Sci USA* 93:13731–13736
 49. Lacapère JJ, Delavoie F, Li H, Péranzi G, Maccario J, Papadopoulos V, Vidic B 2001 Structural and functional study of reconstituted peripheral benzodiazepine receptor (PBR). *Biochem Biophys Res Commun* 284:536–641
 50. West LA, Horvat RD, Roess DA, Barisas GB, Juengel JL, Niswender GD 2001 Steroidogenic acute regulatory protein and peripheral-type benzodiazepine receptor associate at the mitochondrial membrane. *Endocrinology* 142:502–505
 51. Gietz D, St. Jean A, Woods RA, Schiestl RH 1992 Improved method for high efficiency transformation of intact yeast cells. *Nucleic Acids Res* 20:1425
 52. El Hefnawy T, Krawczyk Z, Nikula H, Vihera I, Huhtaniemi I 1996 Regulation of function of the murine luteinizing hormone receptor promoter by *cis*- and *trans*-acting elements in mouse Leydig tumor cells. *Mol Cell Endocrinol* 119:207–217
 53. Yao Z, Drieu K, Szweda LI, Papadopoulos V 1999 Free-radicals and lipid peroxidation do not mediate β -amyloid-induced neuronal cell death. *Brain Res* 847:203–210
 54. Munson PJ, Rodbard D 1980 Ligand: a versatile computerized approach for characterization of ligand-binding systems. *Anal Biochem* 107:220–239
 55. Tasken K, Skalhegg BS, Solberg R, Andersson KB, Taylor SS, Lea T, Blomhoff HK, Jahnsen T, Hansson V 1993 Novel isozymes of cAMP-dependent protein kinase exist in human cells due to formation of RI α -RI β heterodimeric complexes. *J Biol Chem* 268:21276–21283
 56. Levin MC, Fox RJ, Lehky T, Walter M, Fox CH, Flerlage N, Bamford R, Jacobson S 1996 PCR-*in situ* hybridization detection of human T-cell lymphotropic virus type 1 (HTLV-1) tax proviral DNA in peripheral blood lymphocytes of patients with HTLV-1-associated neurologic disease. *J Virol* 70:924–933
 57. Bradford MM 1976 A rapid and sensitive method for the quantitation of microgram quantities of protein utilizing the principle of protein-dye binding. *Anal Biochem* 72:248–254

